Published online 17 May 2011 *Nucleic Acids Research, 2011, Vol. 39, No. 16* ***7329–7335***
doi:10.1093/nar/gkr360

Base pair opening kinetics study of the *aeg*PNA:DNA hydrid duplex containing a site-specific GNA-like chiral PNA monomer

Yeo-Jin Seo[1], Jisoo Lim[2], Eun-Hae Lee[1], Taedong Ok[2], Juyoung Yoon[3], Joon-Hwa Lee[1,*] and Hee-Seung Lee[2,*]

[1]Department of Chemistry and RINS, Gyeongsang National University, Jinju, Gyeongnam 660-701, [2]Molecular-Level Interface Research Center, Department of Chemistry, KAIST, Daejeon 305-701 and [3]Department of Chemistry and Nano Science, Ewha Womans University, Seoul 120-750, Republic of Korea

Received March 10, 2011; Revised April 25, 2011; Accepted April 27, 2011

ABSTRACT

Peptide nucleic acids (PNA) are one of the most widely used synthetic DNA mimics where the four bases are attached to a *N*-(2-aminoethyl)glycine (*aeg*) backbone instead of the negative-charged phosphate backbone in DNA. We have developed a chimeric PNA (*chi*PNA), in which a chiral GNA-like γ^3T monomer is incorporated into *aeg*PNA backbone. The base pair opening kinetics of the *aeg*PNA:DNA and *chi*PNA:DNA hybrid duplexes were studied by NMR hydrogen exchange experiments. This study revealed that the *aeg*PNA:DNA hybrid is much more stable duplex and is less dynamic compared to DNA duplex, meaning that base pairs are opened and reclosed much more slowly. The site-specific incorporation of γ^3T monomer in the *aeg*PNA:DNA hybrid can destabilize a specific base pair and its neighbors, maintaining the thermal stabilities and dynamic properties of other base pairs. Our hydrogen exchange study firstly revealed the unique kinetic features of base pairs in the *aeg*PNA:DNA and *chi*PNA:DNA hybrids, which will provide an insight into the development of methodology for specific DNA recognition using PNA fragments.

INTRODUCTION

Peptide nucleic acids (PNA) are one of the most widely used synthetic DNA mimics where the four bases are attached to a *N*-(2-aminoethyl)glycine (*aeg*) backbone (Figure 1A) instead of the negative-charged phosphate backbone in DNA (1,2). Today, PNAs have been used for various application purposes such as: (i) potential drug candidates for gene therapy; (ii) molecular tools in biotechnology; (iii) lead compounds for the development of gene-targeted drugs; (iv) diagnostic biosensors (3). PNA is capable of sequence-specific recognition to DNA as well as RNA and forms various hybrid complexes such as PNA:PNA, PNA:DNA, PNA:RNA duplexes and PNA:PNA:PNA, PNA:DNA:PNA triplexes (4–8). UV melting studies of PNA hybrids revealed that the PNA sequences can bind to their complementary DNA, RNA and PNA strands with great affinities (5,9–11). Thermodynamic studies revealed that the hybridization of DNA with complementary PNA strand significantly increased the thermal stability of the double helix compared to DNA duplex, mainly due to the lack of interstrand electrostatic repulsion (12–14).

However, drawbacks such as poor cellular uptake, ability to form hybrids with both parallel and antiparallel orientation and similiar binding affinity to DNA/RNA are known to be the subjects for improvement. Especially, the latter two may lead to poor specificity toward the target sequence, which give rise to undesirable effects both in biological and diagnostic applications. Recently, we have developed a structurally simple chiral PNA monomer with thymine base (named γ^3**T**, Figure 1B) and prepared a chimeric PNA (named *chi*PNA, Figure 1C), in which γ^3**T** monomers are incorporated into *aeg*PNA backbone (15). This *chi*PNA displays excellent RNA selectivity as well as antiparallel selectivity compared to *aeg*PNA although the melting temperatures of most *chi*PNA:DNA hybrids are slightly lower than the corresponding *aeg*PNA:DNA hybrids (15). Previous hydrogen exchange

*To whom correspondence should be addressed. Tel: +82 55 772 1490; Fax: +82 55 772 1489; Email: joonhwa@gnu.ac.kr
Correspondence may also be addressed to Hee-Seung Lee. Tel: +82 42 350 2846; Fax: +82 42 350 2810; Email: hee-seung_lee@kaist.ac.kr

The authors wish it to be known that in their opinion, the first three authors should be regarded as joint First Authors.

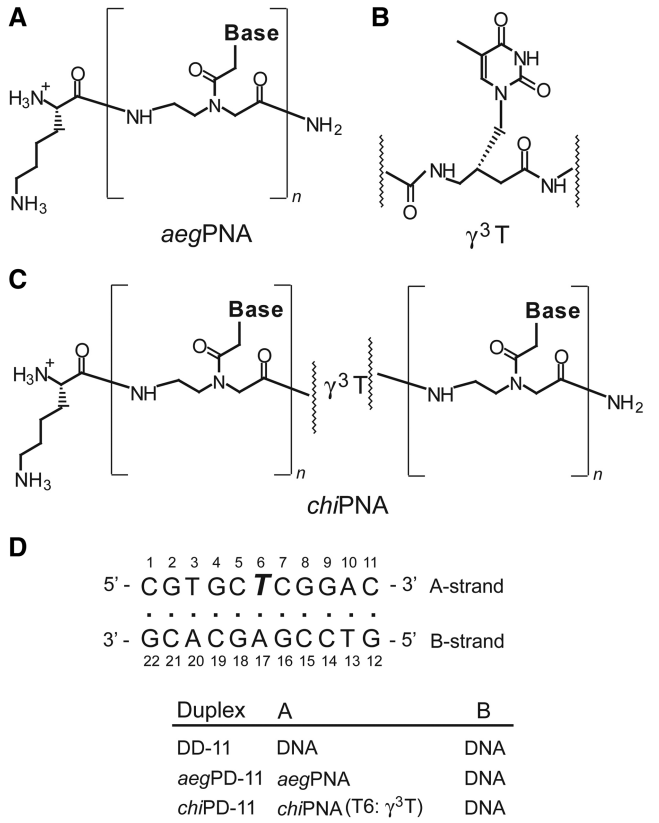

Duplex	A	B
DD-11	DNA	DNA
*aeg*PD-11	*aeg*PNA	DNA
*chi*PD-11	*chi*PNA (T6: γ^3T)	DNA

Figure 1. The chemical structures of (**A**) *aeg*PNA, (**B**) (*R*)-γ^3**T**, (**C**) *chi*PNA with a (*R*)-γ^3**T**. (**D**) Sequence contexts of the duplex samples studied.

study using ammonia reported that the imino protons in the *aeg*PNA:DNA hybrid had similar base pair stabilities but very short base pair lifetimes compared to the corresponding DNA duplex (16). In order to account for the change in thermal stability and base pair dynamics of nucleic acid duplexes upon introduction of a new type of monomer in *aeg*PNA:DNA hybrid, we performed the NMR exchange studies on the: (i) DNA:DNA duplex (DD-11); (ii) *aeg*PNA:DNA hybrid (*aeg*PD-11); or (iii) *chi*PNA:DNA hybrid (*chi*PD-11) which was formed by a single-stranded *aeg*PNA containing a site-specific γ^3**T** and its complementary DNA strand (Figure 1D). These data showed the unique kinetic features of base pairs in the *aeg*PNA:DNA and *chi*PNA:DNA hybrids, which will provide an insight into the development of methodology for specific DNA recognition using PNA fragments.

MATERIALS AND METHODS

Sample preparation

Fmoc-protected *aeg*PNA monomers were purchased from PANAGENE (Daejeon, Korea), where the exocyclic amino groups of **A**, **G**, **C** are Bhoc-protected. The (R)-γ^3**T** PNA monomer was synthesized as described in our previous report (15). The *aeg*PNA and (R)-γ^3**T**–modified *chi*PNA oligomers were synthesized by using standard solid phase Fmoc-chemistry using Peptide synthesizer (ABI 433A, Applied Biosystems Inc., USA). The DNA oligomers were purchased from M-biotech Inc. (Seoul, Korea). The PNA and DNA oligomers were purified by reverse-phase HPLC and desalted using a Sephadex G-25 gel filtration column. The three duplex samples were prepared by dissolving the *aeg*PNA, *chi*PNA and DNA strands with sequence of 5′-CGTGCTCGGAC-3′ (A strand in Figure 1D) and the complementary DNA strand, 5′-GTCCGAGCACG-3′ (B strand in Figure 1D) at a 1:1 stoichiometric ratio in a 90% H_2O/10% D_2O aqueous solution containing 10 mM TRIS-d_{11} (pH 8.0 at 24.2°C) and 100 mM NaCl.

NMR experiments

All NMR experiments were performed on a Varian Inova 600 MHz spectrometer (KAIST, Daejeon) using a HCN triple-resonance probe. One dimensional (1D) NMR data were processed with either the program VNMR J (Varian, Palo Alto) or FELIX2004 (Accelrys, San Diego), whereas 2D data were processed with the program NMRPIPE (17) and analyzed with the program Sparky (18). The apparent longitudinal relaxation rate constants ($R_{1a} = 1/T_{1a}$) of the imino protons were determined by semi-selective inversion recovery 1D NMR experiments. The apparent relaxation rate constant of water (R_{1w}) was determined by a selective inversion recovery experiment, using a DANTE sequence for selective water inversion (19). R_{1a} and R_{1w} were determined by curve fitting of the inversion recovery data to the appropriate single-exponential function. The hydrogen exchange rate constants (k_{ex}) of the imino protons were measured by a water magnetization transfer experiment (19–22). The intensities of each imino proton were measured with 20 different delay times. The k_{ex} for the imino protons were determined by fitting the data to Equation (1):

$$\frac{I_0 - I(t)}{I_0} = 2\frac{k_{ex}}{(R_{1w} - R_{1a})}\left(e^{-R_{1a}t} - e^{-R_{1w}t}\right) \quad (1)$$

where I_0 and $I(t)$ are the peak intensities of the imino proton in the water magnetization transfer experiments at times zero and t, respectively, and R_{1a} and R_{1w} are the apparent longitudinal relaxation rate constants for the imino proton and water, respectively, measured in semi-selective inversion recovery 1D NMR experiments. The formalism of TRIS-catalyzed proton exchange has been previously described in detail in the previous study (19,21,22) and is briefly presented here. The exchange time for the base paired imino proton, τ_{ex} (inverse of k_{ex}), is represented by:

$$\tau_{ex} = \tau_0 + \frac{1}{\alpha K_{op} k_i}\frac{1}{[\mathrm{TRIS}]} \quad (2)$$

where τ_0 is the base pair life time (inverse of opening rate constant, k_{op}), k_i is the rate constant for imino proton transfer, and αK_{op} ($= \alpha k_{op}/k_{cl}$) is the apparent equilibrium constant for base pair opening. The k_i values for

TRIS-catalyzed imino proton transfer are calculated by Equation (3):

$$k_i = \frac{k_{coll}}{1+10^{\Delta pK_a}} \quad (3)$$

where k_{coll} is the collision rate constant for TRIS ($= 1.5 \times 10^9\,s^{-1}$), and ΔpK_a is the pK_a difference between the imino proton (G-H1: 9.24; T-H3: 9.60) and the TRIS base (25°C, 8.15). The actual concentrations of TRIS were calculated using equation $[TRIS] = [TRIS]_{total}/(1+10^{(pKa-pH)})$. Curve fitting the τ_{ex} values of the imino protons as a function of the inverse of [TRIS] with Equation (2) gives the αK_{op} and τ_0 ($= 1/k_{op}$) values.

RESULTS AND DISCUSSION

Temperature dependency of 1D imino proton spectra

Resonance assignments for the imino protons were made by the analysis of NOESY spectra. Figure 2 shows the temperature dependence of 1D imino proton spectra of DD-11, *aeg*PD-11 and *chi*PD-11 duplexes. Most imino resonances are well resolved in the 1D spectra because the nucleotide sequence was designed to minimize overlapping of these resonances. All imino resonances except those of the terminal base pairs and the neighboring A10·T13 base pairs in three duplexes were intact over 25°C (Figure 2), indicating that the three duplexes form stable double helices at room temperature. Interestingly, the melting temperature of *aeg*PD-11 was 10°C higher than those of DD-11 and *chi*PD-11 (Figure 2), which is consistent with the previous thermodynamic studies (12–14). In *chi*PD-11, the T6 and G16 imino resonances have lower melting temperature than those of *aeg*PD-11 (Figure 2). These results clearly demonstrates that the T6·A17 and C7·G16 base pairs and the overall helical structure are destabilized upon the incorporation of γ^3**T** at T6 position into the *aeg*PNA strand.

Hydrogen exchange experiments for imino protons

The hydrogen exchange rate constants (k_{ex}) determined from water magnetization transfer experiment on the imino protons for DD-11, *aeg*PD-11 and *chi*PD-11 duplexes at 15°C (Figure 3) (19–23). Some imino protons show large change in peak intensities as a function of delay time after water inversion (Figure 3). For example, rapidly exchanging imino protons such as T13 in three duplexes and T6 in *chi*PD-11 show negative peaks at delay time of 50 ms (Figure 3), whereas the G8 resonance in DD-11, which is the slowest exchanging imino proton, remains basically unchanged up to 100 ms. The relative peak intensities, $I(t)/I_0$, for the T6 and G16 imino proton resonances of three duplexes are plotted as a function of delay time in Figure 3D and E, respectively. These data were used to determine k_{ex} by fitting Equation (1). The k_{ex} values for individual imino protons in the DD-11, *aeg*PD-11 and *chi*PD-11 duplexes determined at 15°C are shown in Table 1. Many of the imino protons exchanged too slowly to be accurately determined from this NMR hydrogen exchange method ($k_{ex} \leq 1.5\,s^{-1}$) at 15°C because the peak intensities for these protons could be affected by not only solvent exchange but also direct or spin-diffused NOE interaction with water (20).

To further characterize the more stable regions in the three duplexes, the k_{ex} measurements were performed at 25°C. The T13 imino resonances in the three duplexes and T6 imino resonance in *chi*PD-11 were not observed at 25°C, which means the $k_{ex} > 400\,s^{-1}$ (20). Interestingly, the k_{ex} values of the T3 imino protons in *aeg*PD-11 and *chi*PD-11 are 4-fold smaller than that of DD-11 at 25°C. In addition, the central T6 imino proton in *aeg*PD-11 has k_{ex} value of $1.6\,s^{-1}$, which is 24-fold smaller than that of

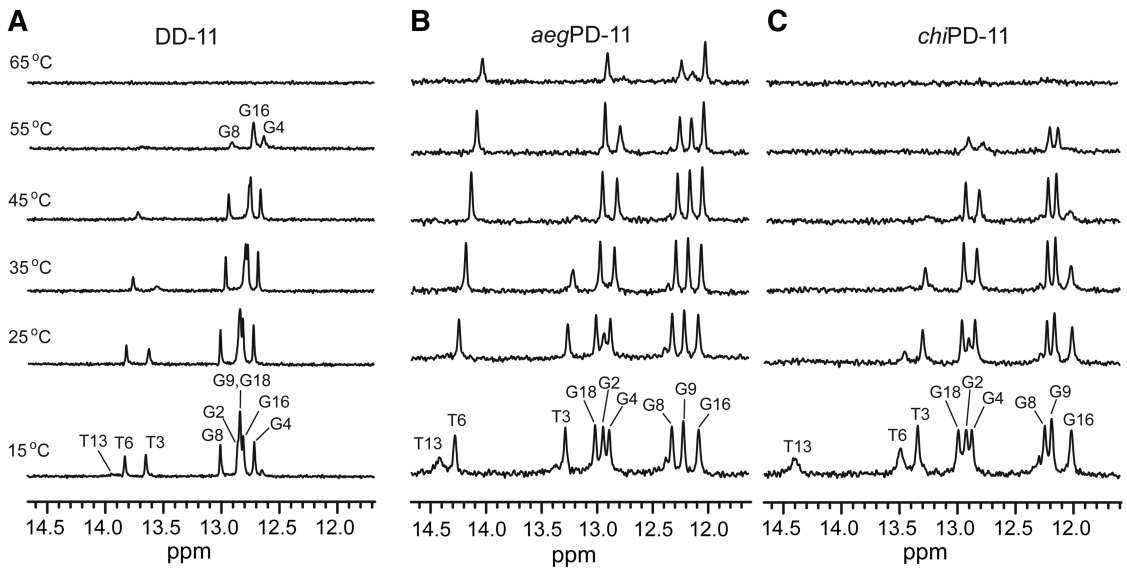

Figure 2. Temperature-dependent 1D imino proton spectra for the (**A**) DD-11, (**B**) *aeg*PD-11, and (**C**) *chi*PD-11 duplexes in a 90% H_2O/10% D_2O solution containing 10 mM TRIS-d_{11} (pH = 8.0, 25°C) and 100 mM NaCl.

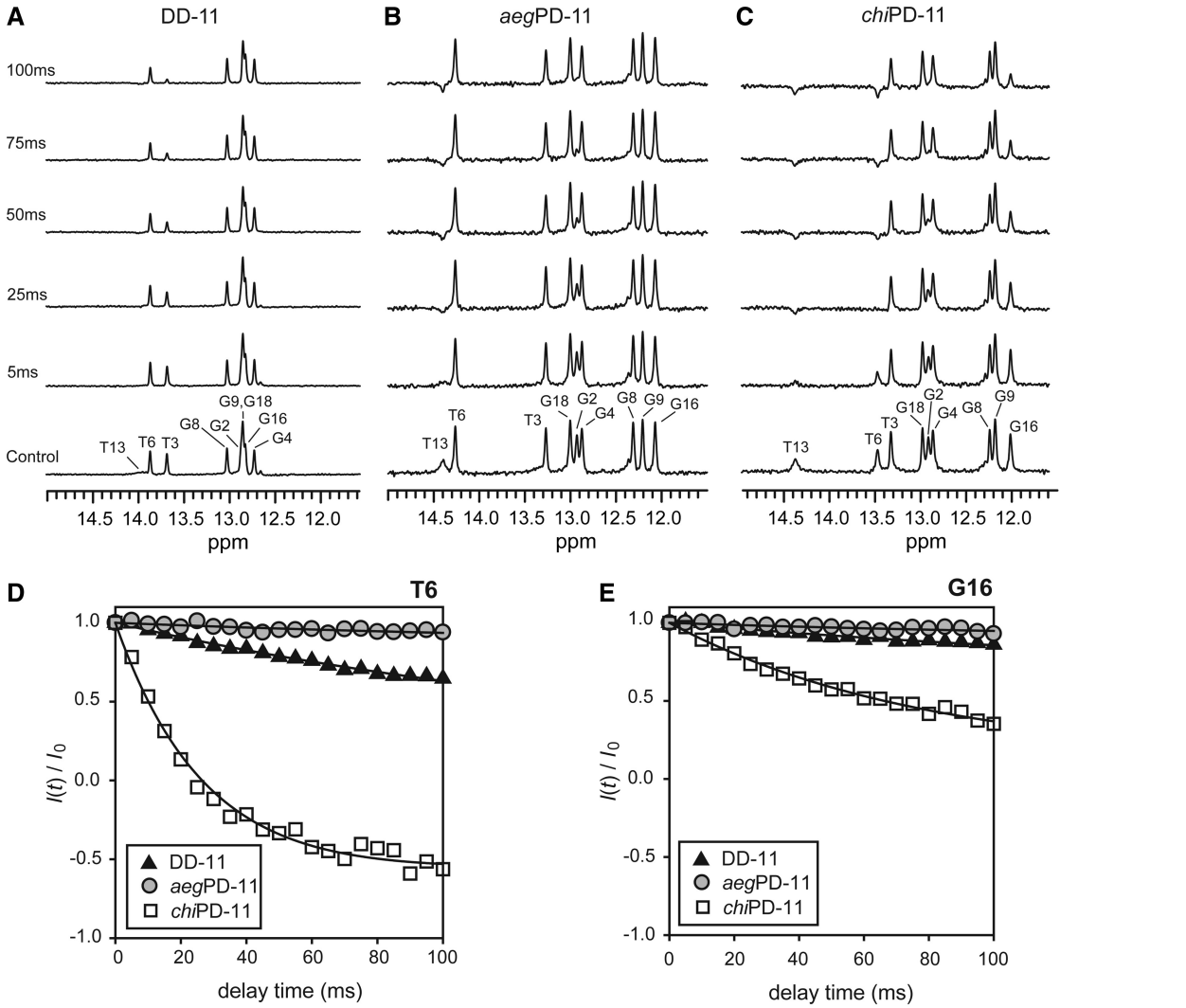

Figure 3. 1D spectra of the water magnetization transfer experiments showing the imino protons of the (**A**) DD-11, (**B**) *aeg*PD-11 and (**C**) *chi*PD-11 duplexes in NMR buffer at 15°C. The relative peak intensities in the spectra, $I(t)/I_0$, as a function of delay time for the (**D**) T6 and (**E**) G16 imino protons in the DD-11 (closed triangle), *aeg*PD-11 (gray circle), and *chi*PD-11 (open square) duplexes at 15°C. Solid lines indicate the best fitting of these data using Equation (1).

Table 1. The hydrogen exchange rate constants of the imino protons, k_{ex} (s^{-1}), for the DD-11, *aeg*PD-11 and *chi*PD-11 duplexes

Imino	15°C[a]			25°C[b]		
	DD-11	*aeg*PD-11	*chi*PD-11	DD-11	*aeg*PD-11	*chi*PD-11
G2	1.5 ± 0.3[c]	7.3 ± 0.7	7.8 ± 0.8	4.1 ± 0.9[c]	15.9 ± 8.0	n.d.[d]
T3	6.6 ± 0.4	1.7 ± 0.6	1.6 ± 1.6	54.0 ± 3.1	13.6 ± 1.5	14.0 ± 2.5
G4	≤1.5	≤1.5	2.0 ± 0.8	≤1.5	≤1.5	3.0 ± 1.3
G18	1.5 ± 0.3[c]	≤1.5	1.6 ± 0.6	4.1 ± 0.9[c]	≤1.5	4.0 ± 0.9
T6	2.4 ± 0.4	≤1.5	29.8 ± 2.3	38.8 ± 1.3	1.6 ± 0.7	>400
G16	≤1.5	≤1.5	5.6 ± 0.8	≤1.5	≤1.5	53.6 ± 1.5
G8	≤1.5	≤1.5	≤1.5	≤1.5	1.6 ± 0.7	2.4 ± 1.0
G9	1.5 ± 0.3[c]	≤1.5	≤1.5	4.1 ± 0.9[c]	1.5 ± 0.6	2.0 ± 1.1
T13	121 ± 21	84.3 ± 9.2	74.1 ± 5.8	>400	>400	>400

[a]Sample conditions: pH = 8.0, 100 mM NaCl, $[TRIS]_{total}$ = 10 mM, 15°C.
[b]Sample conditions: pH = 8.0, 100 mM NaCl, $[TRIS]_{total}$ = 40 mM, 25°C.
[c]The G2, G9 and G18 imino proton resonances overlap in the DD-11 duplex.
[d]The G2 imino proton resonance shows severe line-broadened in the *chi*PD-11 duplex.

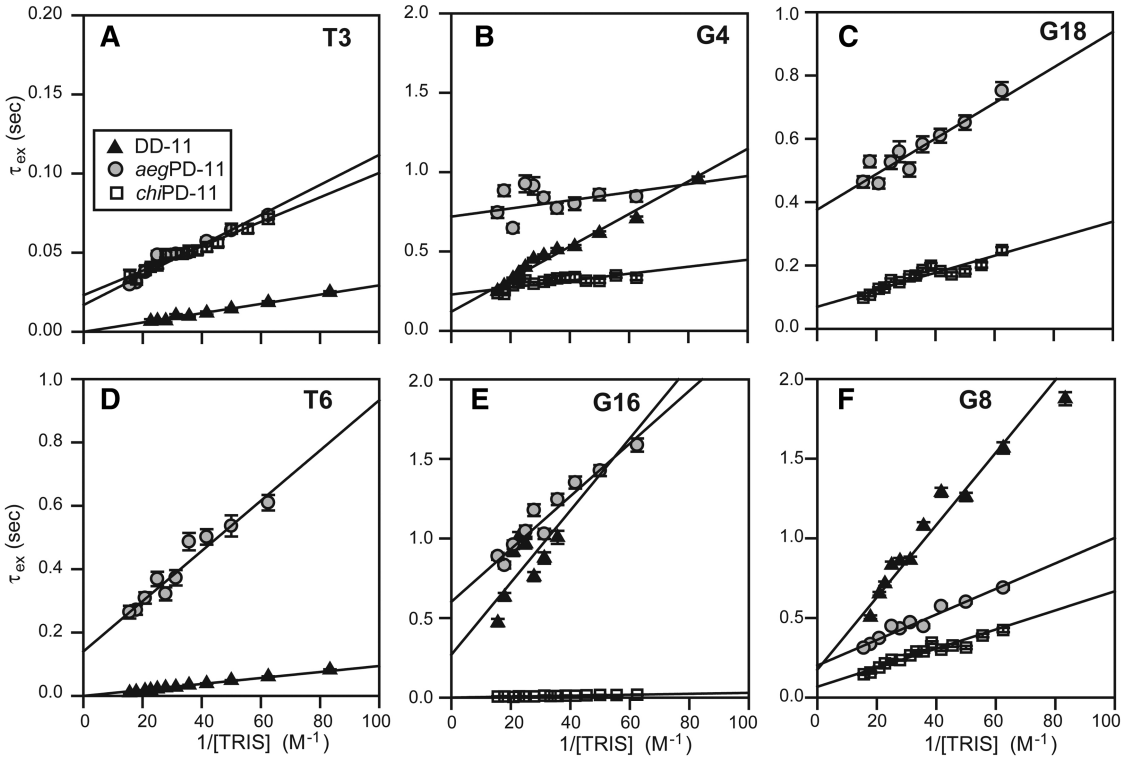

Figure 4. The hydrogen exchange times (τ_{ex}) of the (**A**) T3, (**B**) G4, (**C**) G18, (**D**) T6, (**E**) G16 and (**F**) G8 imino protons of the DD-11 (closed triangle), *aeg*PD-11 (gray circle) and *chi*PD-11 (open square) duplexes as a function of the inverse of TRIS concentration at 25°C. Solid lines indicate the best fitting of these data using Equation (2).

the DD-11 duplex at 25°C. These results demonstrate that the hybridization of DNA with *aeg*PNA strand significantly reduces the k_{ex} values for the imino protons of the A·T base pairs but has little effects on the G imino protons (Table 1). However, the T6 imino resonance in *chi*PD-11 was not observed, which means that its k_{ex} value at 25°C is larger than 400 s^{-1} (20). At 15°C, the peak intensity of T6 imino proton in *chi*PD-11 depends more significantly on delay time compared to DD-11 and *aeg*PD-11 (Figure 3D), demonstrating that the specific base pair in *chi*PNA:DNA is more unstable than the corresponding *aeg*PNA:DNA and DNA:DNA base pairs. This instability also affects the k_{ex} value of the neighboring base pairs. For example, the G16 imino proton in *chi*PD-11 has k_{ex} value of 53.6 s^{-1}, which is 36-fold larger than the k_{ex} values of DD-11 and *aeg*PD-11 at 25°C.

Base pair opening kinetics

The apparent equilibrium constants (αK_{op}) for base pair opening in the DD-11, *aeg*PD-11 and *chi*PD-11 duplexes can be determined by base-catalyzed imino proton exchange measurements. Ammonia is the most commonly used base catalyst in thermodynamic and kinetic study for base pair opening in the nucleic acid duplexes. However, ammonia causes severe line broadening of the imino proton resonances in very unstable nucleic acid duplexes at high temperature because of its high catalytic efficiency. For example, some imino protons in the P1 duplex of *Tetrahymena* ribozyme, containing a central G·U wobble pair, exhibited substantial line broadening when $[NH_3] > 30$ mM; thus, the αK_{op} for opening of these base pairs could not be determined by ammonia catalyst (19). In the case of *chi*PD-11, T6 imino proton resonance were not observed even at 25°C and this instability also affects the k_{ex} value of the neighboring G16 imino proton. Therefore, TRIS base was thought to be the most suitable catalyst for the hydrogen exchange studies to examine the effect of the incorporation of a site-specific γ^3**T** monomer into the *aeg*PNA:DNA hybrid duplex. The k_{ex} ($= 1/\tau_{ex}$) for each imino proton in the DD-11, *aeg*PD-11 and *chi*PD-11 duplexes was measured at 25°C as a function of the TRIS concentration (Figure 4). From these data, the equilibrium constants for base pair opening (αK_{op}) and the base pair lifetimes ($\tau_0 = 1/k_{op}$) of the three duplexes were determined by curve fitting using Equation (2) (Figure 4). In DD-11, the three G·C base pairs determined here have $\alpha K_{op} \leq 1 \times 10^{-6}$ and $\tau_0 > 100$ ms (Table 2). These data can be used to calculate an apparent lifetime for base pair opening ($\alpha\tau_{open} = \alpha/k_{cl}$) of 70–100 ns (using $\alpha\tau_{open} = \tau_0 \alpha K_{op}$). However, the A·T base pairs have much larger αK_{op} values (T3·A20: 67×10^{-6} and T6·A17: 21×10^{-6}) than the G·C base pairs and their base pair lifetimes could not be determined ($\tau_0 < 1$ ms; Table 2 and Figure 4).

These data were used to compare the effect of the hybridization of DNA with *aeg*PNA on the base pair

Table 2. The equilibrium constants for base pair opening (αK_{op}), base pair lifetimes (τ_0) and apparent lifetimes for base pair opening ($\alpha\tau_{open}$) of the DD-11, *aeg*PD-11 and *chi*PD-11 duplexes determined by TRIS-catalyzed NMR exchange experiments at 25°C[a]

Parameter	Base pair	DD-11	*aeg*PD-11	*chi*PD-11
αK_{op} ($\times 10^{-6}$)	T3·A20	67 ± 3	21 ± 2	26 ± 2
	G4·C19	0.9 ± 0.1	3.5 ± 3.9	4.1 ± 1.0
	C5·G18	n.d.[b]	1.6 ± 0.2	3.3 ± 0.4
	T6·A17	21 ± 1	2.5 ± 0.2	n.a.[c]
	C7·G16	0.4 ± 0.2	0.5 ± 0.1	30 ± 3
	G8·C15	0.4 ± 0.1	1.1 ± 0.1	1.5 ± 0.1
	G9·C14	n.d.[b]	1.1 ± 0.1	1.4 ± 0.1
τ_0 (ms)	T3·A20	<1	17 ± 2	23 ± 2
	G4·C19	120 ± 20	720 ± 88	229 ± 17
	C5·G18	n.d.[b]	376 ± 25	69 ± 9
	T6·A17	<1	140 ± 21	n.a.[c]
	C7·G16	270 ± 234	602 ± 47	<1
	G8·C15	175 ± 53	201 ± 18	68 ± 14
	G9·C14	n.d.[b]	171 ± 7	87 ± 14
$\alpha\tau_{open}$ (ns)	T3·A20	<10	350 ± 73	589 ± 79
	G4·C19	100 ± 24	2520 ± 3130	936 ± 289
	C5·G18	n.d.[b]	600 ± 124	232 ± 57
	T6·A17	<10	347 ± 83	n.a.[c]
	C7·G16	107 ± 139	325 ± 56	10 ± 29
	G8·C15	69 ± 26	225 ± 35	101 ± 28
	G9·C14	n.d.[b]	190 ± 15	125 ± 28

[a]Parameters used in the calculations: $k_{coll} = 1.5 \times 10^9$ (s^{-1}), pK_a(G-H1) = 9.24, pK_a(T-H3) = 9.60, pK_a(TRIS, 25°C) = 8.15; Sample conditions: pH = 8.0, 100 mM NaCl, $[TRIS]_{total}$ = 10–300 mM, 25°C. The actual concentrations of TRIS were calculated using equation $[TRIS] = [TRIS]_{total}/(1 + 10^{(pKa\text{-}pH)})$.
[b]Not determined because the G18 imino proton resonance overlaps with G9 imino proton resonance.
[c]No resonances.

stabilities (Figure 4). In *aeg*PD-11, as expected from the k_{ex} data, the αK_{op} values of the T3·A20 and T6·A17 base pairs are 3- and 8-fold smaller than those of DD-11, respectively (Figure 4A and D; Table 2). This means that the A·T base pairs in the *aeg*PNA:DNA hybrid are more stable than those of the corresponding DNA duplex. However, the G4·C19 and G8·C15 base pairs in *aeg*PD-11 have larger αK_{op} values than those of DD-11 (Figure 4B and F; Table 2). These results indicate that the PNA–DNA hybridization, even though some G·C base pairs are slightly destabilized, stabilizes the A·T base pairs and increases the overall thermal stability of the *aeg*PNA:DNA hybrid, compared to the corresponding DNA duplex. These results were consistent with the previous hydrogen exchange study using ammonia in which the T·A base pairs in the *aeg*PNA:DNA hybrid had 3 to 4 times smaller αK_{op} values, but the αK_{op} of the G·C base pairs were 2- to 3-fold larger than those of the corresponding DNA duplex at various temperatures (16).

In Figure 4, the slope of the linear correlation between τ_{ex} ($= 1/k_{ex}$) of the imino proton and inverse of TRIS concentration is $1/(k_i \alpha K_{op})$ and the *y*-intercept is τ_0 [see Equation (2)]. The more stable T3·A20 base pair in *aeg*PD-11 have both a larger slope (smaller αK_{op}) and a larger *y*-intercept (longer τ_0) than those of DD-11 in this plot (Figure 4A), demonstrating that these base pairs in the *aeg*PNA:DNA hybrid are opened much more slowly compared to the DNA duplex. The similar effects are also observed in the T3·A20 base pairs in *aeg*PD-11 (Figure 4D). Surprisingly, the G4·C19 base pair of *aeg*PD-11 has significantly a larger *y*-intercept (longer τ_0) than that of DD-11, in spite of its instability (Figure 4B). Contrary to our results, the previous ammonia-catalyzing exchange study showed that lifetimes (τ_0) for both T·A and G·C base pairs in the *aeg*PNA:DNA hybrid were much shorter ($\leq$1 ms even at 10°C) than those of the corresponding DNA duplex, indicating extremely fast base pair opening/closing (16). However, the previous study had been performed for relatively unstable duplexes, which contained six T·A base pairs in decamer duplex, by using strong catalyst, ammonia at pH = 8.8. These experimental conditions could make imino proton exchanges more rapid for the DNA and *aeg*PNA:DNA hybrid duplexes. Consequently, the base pair lifetimes (τ_0) may not be correctly determined by ammonia catalyst for the *aeg*PNA:DNA hybrid, although the previous study provided the αK_{op} value for each base pair and the important information about the base pair stabilities in the *aeg*PNA:DNA hybrid. In our current, we could show more clearly the unique features of base pair opening in *aeg*PNA:DNA hybrid, in which most base pairs are opened and reclosed much more slowly than those of the corresponding DNA duplex.

In *chi*PD-11, the αK_{op} for the T6·A17 base pair could not be determined because of the severe line-broadening of the T6 imino protons, indicating that the specific base pair (γ^3**T**·A17) in *chi*PNA:DNA base pair is much more unstable than the corresponding pairs in *aeg*PNA:DNA and DNA:DNA duplexes. This difference in the base pair stability between *aeg*PNA:DNA and *chi*PNA:DNA base pairs also affects the stabilities of the neighboring base pairs. The αK_{op} of the C7·G16 base pair [3′-side neighbor of γ^3**T** (T6)] in *chi*PD-11 is about 60-fold larger than that of *aeg*PD-11 (Table 2). Also, its base pair lifetime could not be determined, meaning that $\tau_0 < 1$ ms. The C5·G18 base pair (the 5′-side neighbor) has only 2-fold larger αK_{op} and a 5-fold shorter τ_0 than those of *aeg*PD-11 (Table 2), which means that the γ^3**T**·A17 base pairing in the *chi*PNA:DNA hybrid leads to great destabilization and fast opening of the neighoring base pairs in an asymmetric manner. In Figure 4, the G4·C19 and G8·C15 base pairs of *chi*PD-11 have similar slopes but smaller *y*-intercepts than those of DD-11 in the plots. This means that the γ^3**T**·A17 base pair does not affect on the thermal stabilities of next neighboring base pairs but decreases their base pair lifetimes. The T3·A20 base pair in *chi*PD-11 has the same αK_{op} and τ_0 values with those of *aeg*PD-11 (Table 2), indicating that the γ^3**T**·A17 base pair does not affect the thermal stability of this base pair as well as its base pair opening property.

SUMMARY

The *aeg*PNA:DNA hybrid is much more stable duplex and is less dynamic compared to DNA duplex, meaning that base pairs are opened and reclosed much more slowly.

The site-specific incorporation of γ^3**T** monomer in the *aeg*PNA:DNA hybrid can destabilize a specific base pair and its neighbors, maintaining the thermal stabilities and dynamic properties of other base pairs. Our hydrogen exchange study firstly revealed the unique kinetic features of base pairs in the *aeg*PNA:DNA and *chi*PNA:DNA hybrids, which will provide an insight into the development of methodology for specific DNA recognition using PNA fragments.

ACKNOWLEDGEMENTS

We thank Dr Sung Jae Cho and Prof. Byong-Seok Choi for supporting NMR experiments.

FUNDING

Basic Research Promotion Fund (No. KRF-205-2005-1-C00043); National Research Foundation of Korea (NRF) grants funded by the Korean government (MEST) (No. 2011-0001318; 2010-0014199; NRF-C1ABA001-2010-0020480); Next-Generation BioGreen 21 Program, Rural Development Administration, Korea (SSAC, No. PJ008109). Funding for open access charge: National Research Foundation of Korea.

Conflict of interest statement. None declared.

REFERENCES

1. Nielsen,P.E., Egholm,M., Berg,R.H. and Buchardt,O. (1991) Sequence-selective recognition of DNA by strand displacement with a thymine-substituted polyamide. *Science*, **254**, 1497–1500.
2. Egholm,M., Buchardt,O. and Nielsen,P.E. (1992) Peptide nucleic acids (PNA). Oligonucleotide analogs with an achiral peptide backbone. *J. Am. Chem. Soc.*, **114**, 1895–1897.
3. Ray,A. and Nordén,B. (2000) Peptide nucleic acid (PNA): its medical and biotechnical applications and promise for the future. *FASEB J.*, **14**, 1041–1060.
4. Rasmussen,H., Kastrup,J.S., Nielsen,J.N., Nielsen,J.M. and Nielsen,P.E. (1997) Crystal structure of a peptide nucleic acid (PNA) duplex at 1.7 Å resolution. *Nat. Struct. Biol.*, **4**, 98–101.
5. Brown,S.C., Thomson,S.A., Veal,J.M. and Davis,D.G. (1994) NMR solution structure of a peptide nucleic acid complexed with RNA. *Science*, **265**, 777–780.
6. Eriksson,M. and Nielsen,P.E. (1996) Solution structure of a peptide nucleic acid-DNA duplex. *Nat. Struct. Biol.*, **3**, 410–413.
7. Petersson,B., Nielsen,B.B., Rasmussen,H., Larsen,I.K., Gajhede,M., Nielsen,P.E. and Kastrup,J.S. (2005) Crystal structure of a partly self-complementary peptide nucleic acid (PNA) oligomer showing a duplex-triplex network. *J. Am. Chem. Soc.*, **127**, 1424–1430.
8. Betts,L., Josey,J.A., Veal,J.M. and Jordan,S.R. (1995) A nucleic acid triple helix formed by a peptide nucleic acid-DNA complex. *Science*, **270**, 1838–1841.
9. Egholm,M., Buchardt,O., Christensen,L., Behrens,C., Freier,S.M., Driver,D.A., Berg,R.H., Kim,S.K., Nordén,B. and Nielsen,P.E. (1993) PNA hybridizes to complementary oligonucleotides obeying the Watson-Crick hydrogen-bonding rules. *Nature*, **365**, 566–568.
10. Wittung,P., Nielsen,P.E., Buchardt,O., Egholm,M. and Nordén,B. (1994) DNA-like double helix formed by peptide nucleic acid. *Nature*, **368**, 561–563.
11. Tomac,S., Sarkar,M., Ratilainen,T., Wittung,P., Nielsen,P.E., Nordén,B. and Gräslund,A. (1996) Ionic effects on the stability and conformation of peptide nucleic acid complexes. *J. Am. Chem. Soc.*, **118**, 5544–5552.
12. Schwarz,F.P., Robinson,S. and Butler,J.M. (1999) Thermodynamic comparison of PNA/DNA and DNA/DNA hybridization reactions at ambient temperature. *Nucleic Acids Res.*, **27**, 4792–4800.
13. Chakrabarti,M.C. and Schwarz,F.P. (1999) Thermal stability of PNA/DNA and DNA/DNA duplexes by differential scanning calorimetry. *Nucleic Acids Res.*, **27**, 4801–4806.
14. Ratilainen,T., Holmen,A., Tuite,E., Nielsen,P.E. and Norden,B. (2000) Thermodynamics of sequence-specific binding of PNA to DNA. *Biochemistry*, **39**, 7781–7791.
15. Ok,T., Lee,J., Jung,C., Lim,J., Park,C.M., Lee,J.-H., Park,H.G. and Lee,H.-S. (2011) GNA/aegPNA chimera loaded with RNA binding preference. *Chem. Asian J.*, doi:10.1002/asia.201100003.
16. Leijon,M., Sehlstedt,U., Nielsen,P.E. and Gräslund,A. (1997) Unique base-pair breathing dynamics in PNA-DNA hybrids. *J. Mol. Biol.*, **271**, 438–455.
17. Delaglio,F., Grzesiek,S., Vuister,G.W., Zhu,G., Pfeifer,J. and Bax,A. (1995) NMRPipe: a multidimensional spectral processing system based on UNIX pipes. *J. Biomol. NMR*, **6**, 277–293.
18. Goddard,T.D. and Kneller,D.G. (2003) *SPARKY 3*. University of California, San Francisco, CA.
19. Lee,J.-H. and Pardi,A. (2007) Thermodynamics and kinetics for base-pair opening in the P1 duplex of the *Tetrahymena* group I ribozyme. *Nucleic Acids Res.*, **35**, 2965–2974.
20. Lee,J.-H., Jucker,F. and Pardi,A. (2008) Imino proton exchange rates imply an induced-fit binding mechanism for the $VEGF_{165}$-targeting aptamer, Macugen. *FEBS Lett.*, **582**, 1835–1839.
21. Bang,J., Bae,S.-H., Park,C.-J., Lee,J.-H. and Choi,B.-S. (2008) Structural and dynamics study of DNA dodecamer duplexes that contain un-, hemi-, or fully methylated GATC sites. *J. Am. Chem. Soc.*, **130**, 17688–17696.
22. Bang,J., Kang,Y.-M., Park,C.-J., Lee,J.-H. and Choi,B.-S. (2009) Thermodynamics and kinetics for base pair opening in the DNA decamer duplexes containing cyclobutane pyrimidine dimer. *FEBS Lett.*, **583**, 2037–2041.
23. Guéron,M. and Leroy,J.L. (1995) Studies of base pair kinetics by NMR measurement of proton exchange. *Methods Enzymol.*, **261**, 383–413.